Journal of Medical Systems (2019) 43: 203
https://doi.org/10.1007/s10916-019-1324-3

IMAGE & SIGNAL PROCESSING

Segmentation and Boundary Detection of Fetal Kidney Images in Second and Third Trimesters Using Kernel-Based Fuzzy Clustering

S. Meenakshi[1] · M. Suganthi[1] · P. Sureshkumar[2]

Received: 8 January 2019 / Accepted: 3 May 2019 / Published online: 27 May 2019

Abstract
Organ segmentation is an important step in Ultrasound fetal images for early prediction of congenital abnormalities and to estimate delivery date. In many applications of 2D medical imaging, they face problems with speckle noise and object contours. Frequent scanning of fetal leads to clinical disturbances to the fetal growth and the quantitative interpretation of Ultrasonic images also a difficult task compared to other image modalities. In the present work a three-stage hybrid algorithm has been developed to segment the US fetal kidney images for the detection of shape and contour. At the first stage the hybrid Mean Median (Hybrid MM) filter is applied to reduce the speckle noise. Then a kernel based Fuzzy C - means clustering is used to detect the shape and contour. Finally, the texture features are obtained from the segmented images. Based on the obtained texture features, the abnormalities are detected. The Gaussian Radial basis function provides an accuracy of 80% at the second and third trimesters with weighted constant ranging from 4 to 8, compared to other global kernel functions. Similarly the proposed method has an accuracy of 86% with compared to other FCM techniques.

Keywords Hybrid MM Filter · KFCM · Dice coefficient · Jaccard index

Introduction

Segmentation plays a key role in medical imaging and abnormality detection techniques. The appropriate imaging techniques such as Computer Tomography (CT), Magnetic Resonance Imaging (MRI) and Ultrasound (US) play a major role in projecting, and early detection of many abnormalities, prediction of delivery time etc., in combination with a set of powerful image segmentation and classification methods. Ultrasound (US) Imaging is a cost-effective real-time imaging, provides high spatial resolution, also no risk for mother and fetus and hence US images are predominant in obstetrics and gynecology. It is an operator dependent technique and the performance is limited by image resolution and fetal position.

This article is part of the Topical Collection on *Image and Signal Processing*

✉ S. Meenakshi
meenakshisece@gmail.com

[1] Mahendra College of Engineering, Salem 636106, India

[2] Mahendra Engineering College, Namakkal 637503, India

The dependence of fetal renal abnormalities on gestational age is presented in [1] and the results shows that only 56 percentages of anomalies have been determined at 24 weeks hence a precious technique is needed for better prediction. Recent studies indicate that up to 1 per 6000 pregnancies are identified in congenital disorders with obstructive uropathies contributing to 24% of prenatal detection of congenital abnormalities. In pregnancy, second and third trimesters play a key role in the detection and monitoring of fetal and parental health status [2].

The second and third trimester ranges from the 13th week to 36th week where several scans related to heart, lungs, kidney and brain are made to assess and ensure the healthy development of organs of the fetus. The second and third trimester ultrasound fetal image is shown in Fig. 1a and b.

The use of fetal Magnetic Resonance Imaging (MRI) for the prediction of central nervous system anomalies at second trimester has been illustrated in [3]. However, this method has limitations in lacking of equipment and experts, also it has time and cost complexity. The MRI causes damage to the fetus up to 1.5 Tesla. Hence it is advisable to use Ultrasonography for fetal growth detection.

Fetal kidney can be visualized only from 9th week and completely seen in 12th week through trans-abdominal and

(a) 15th week 3D fetal US Image

(b) 26th week 3D fetal US Image

Fig. 1 **a** 26th week 3D Fetal US Image, **b** 15th week 3D Fetal US Image

transvaginal sonography in [4]. Using appropriate segmentation methods, several abnormalities could be detected at the early stage of second trimester to avoid future fatal complications. Some of the abnormalities that may be detected include bilateral renal agenesis, infantile polycystic kidney disease, multicyclic dysplastic kidney disease and hydrophrosis etc. The first abnormality can be detected in the second trimester characterized by an absence of bladder and absence of fetal kidneys in the scanned image. In the next case, the polycystic disease is prevalent at a rate of 1:50000 cases characterized by enlarged kidneys. The third disease is characterized by cystic tubules with cysts determining the size of the fetal kidneys.

Normal errors that occur during the Ultrasound diagnosis of kidneys have been illustrated in [5]. The main sources of errors are experience of the Ultra-sonographer, poor class of the scanner etc., Also, during the examination due to small size of kidneys the clear visualization is impossible due to obesity, kidney localization and intestinal gas.

The major problem in the detection features faced by the doctor is Speckle noise introduced in the ultrasound image due to ultrasound echoes. It is a complex phenomenon and degrades the quality of the image. Hence reduction of speckle noise is very much necessary to detect the fine details of an image. The reductions of speckle noise with different kinds of filter for various kinds of images have been described in [6]. It is observed that the Median filter provides a best result for ultrasound kidney images. Wan Mahani Hafizah et al., [7] applied various spatial domain filtering techniques for the enhancement of ultrasound kidney images. It has been concluded that Median filter is best useful for enhancing kidney images as well as preserving edges.

The performance comparison of different types of filters for speckle noise removal has been presented in [8] for remote sensing applications. The application of mean filter minimizes the variance and achieves good results for an optimal additive Gaussian noise. However, the multiplicative property of speckle noise needs a filter for non-Gaussian noise. Hence order statistics filter like median filter and adaptive median filters have been applied for the removal of speckle noise. It shows that adaptive median filter works well for speckle noise.

The different methods used for the removal of noise in ultrasound images have been given in [9]. The performance parameters such as Signal-to-Noise Ratio (SNR), Root Mean Square Error (RMSE) and Mean Absolute Error (MAE) are used for comparison. It is identified that the scalar filters have superior performance in removing high frequency noise but fails to preserve the edges. Whereas the adaptive filters preserve the details but requires more computation time.

There are three different noise removing algorithms obtained by combining mean and median filtering for MRI and Ultrasound medical images and their performance is presented for noiseless images in [10]. The method works better with other methods by retaining the structural details and the function of smoothing filter is suffered by blurring effect.

Karamjeet Singh et al., [11] proposed a hybrid denoising approach by combining local and nonlocal information in Ultrasound images. Initially by using local statistics the effect of speckle noise is removed and speckle reducing bilateral filter is used to reduce the noise further. Finally, the edges are preserved using post processing algorithm. It shows that the edge preserving capability of the hybrid method is superior to other methods.

The different methods used for medical image segmentation has been analyzed [12]. The pixel and region-based thresholding techniques are simple but have fewer applications. Fuzzy C Means algorithm gives good result for overlapping data and sensitive to initial number of clusters. Neural Network algorithms are feasible for texture-based segmentation. By integrating one method with other the performance of the method has been enhanced.

Mahdi Marsousi et al., [13] developed an automated computer aided kidney diagnosis and segmentation from 3D ultrasound kidney images using probabilistic kidney shape model. This technique needs a prior knowledge about kidney shapes, and the performance is sensitive to the width of Gaussian filter.

The segmentation of kidney images from Ultrasound images by combining texture features and shape prior method has been proposed in [14]. With the use of Gabor filters and two-sided convolution strategy the textured objects with incomplete boundaries can be easily eliminated. This provides a method with the ability to deal with textured objects with incomplete boundaries. However, it needs a manual method for placing initial segmenting curves and smoothing the speckle noise is also a complex process.

Segmentation of CT kidney images using Fuzzy C-means with spatial information and Improved Grow Cut (IGC) has been proposed in [15]. The IGC algorithm automatically generates the seed labels and uses the continuity of CT sequences to improve the efficiency. This method provides a specificity of 99.82% and sensitivity of 95.46% for abdominal CT images.

The segmentation of brain tissues from MRI brain images developed in [16] using Kernelized Fuzzy 픠-Means Clustering (KFCM) and Independent Component Analysis (ICA). The skull regions were initially removed by applying thresholding and kernel induced distance in KFCM determines the brain tissues in a reliable manner. The accuracy of this method is evaluated using similarity measures.

Accurate liver segmentation from CT images with the help of adaptive thresholding, Kernel Fuzzy C-Means (KFCM) clustering for detection of liver tumor has been explained [17]. Initially 3D Gaussian filter is applied to eliminate the noises. The adaptive thresholding and kernel fuzzy C-means has been used to separate the liver tumor. The kernel function used is Gaussian Radial Basis Function (GRBF) kernel and the results were compared with FCM. It shows the KFCM has superior performance with FCM.

Bezdek [18] proposed the Fuzzy C- means (FCM), algorithm, which is most widely used for image segmentation, feature analysis, clustering and classification, because of its robust characteristics. The main drawback of FCM algorithm wrongly classifies the noisy pixels if the image is heavily affected by noise and it is effective only if the cluster shape is crisp or spherical. The detailed study and comparison of some Fuzzy K-means algorithms has been presented with and without noise components in [19]. The performance can be analyzed both quantitatively and qualitatively. It has been concluded that KFCM shows better performance and the execution time is also less compared to other kernel based FCM techniques.

Deepa Parasar et al., [20] proposed a segmentation algorithm for foetus Ultrasound images using K-means clustering algorithm and fuzzy filter. The particle swarm optimization in K-means clustering partitioning the foetus Ultrasonic images into multiple segments. However, it needs a better enhancement technique for preserving the edges.

A semi-automatic segmentation method by utilizing the Gradient Vector Force (GVF) to determine the boundaries of fetal kidney image has been proposed by Arpana M. Kop et al., [21]. The method is applied for left as well as right side kidneys. To perform classification on this method also needs texture, edge curvature and shape of the object. A novel Kernelized Type-2 Fuzzy c- Means (KT2FCM) technique is for synthetic and Real CT scan and MR images medical images have been illustrated in [22]. Here the kernel induced metric in the data space to replaces the Euclidean norm metric. The results were compared with FCM and it provides better segmentation.

Shape based kidney segmentation method by considering the kidney in black and white region and back ground separately in [23]. Shape prior model is applied to smooth the boundary of a kidney image. The estimated values were compared with the edge-based level set model. It needs an alignment model to find the initial data set due to diversity in patient kidney shapes. Different algorithms are implemented in various cases and by comparing all those researches work a conclusion made in the proposed model.

Proposed Work

An efficient method for early detection of congenital abnormalities and gestational age by analyzing fetal kidney images could be done by incorporating a precise preprocessing and segmentation algorithm. The present work combines the clustering and texture analysis method to effectively segment the second and third trimester US images. A simple scheme of proposed research flow is given in Fig. 2.

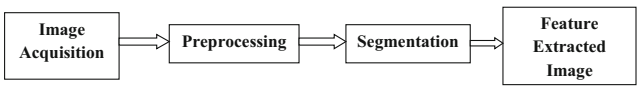

Fig. 2 Simple scheme of Segmentation of Images

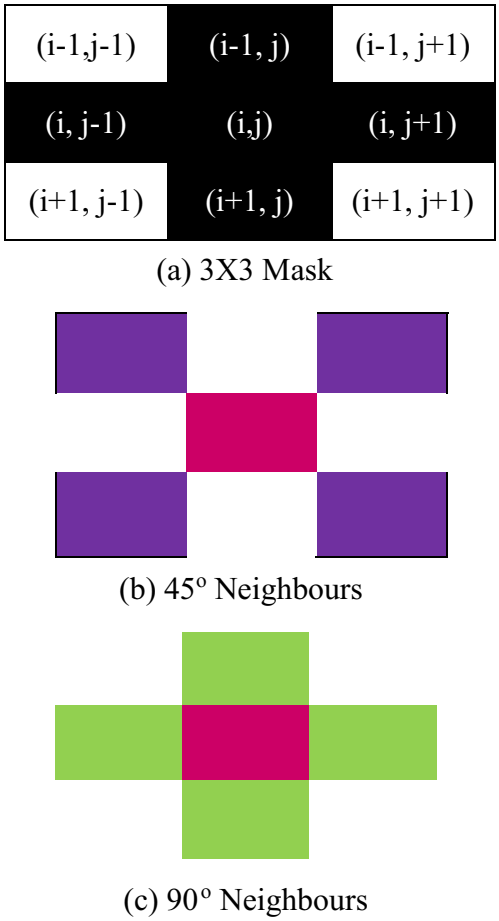

Fig. 3 **a** 3X3 Mask, **b** 45° Neighbours, **c** 90° Neighbours

From the Fig. 2, it is seen that the input image acquired from Ultrasound or Sonography is preprocessed as they may susceptible to noise from the imaging device. Most of the noises associated in medical images are multiplicative in nature. A suitable filter mask may be used to filter out the noise components. It is to be noted that speckle noise is multiplicative and usage of conventional filters like mean, median filters, and Gaussian filters may also help to remove the noise but will not aid in preserving the edges.

Since the Speckle noise contains high frequency components, a low pass filter is initially needed to remove the high frequency noise. The fetal kidney images doesn't have any bright bones it needs a specific algorithm to preserve the edges. Hence a specialized filter has to be applied to the input US image which reduces speckle as well as preserves the edges. In general, a speckle noise model is represented as

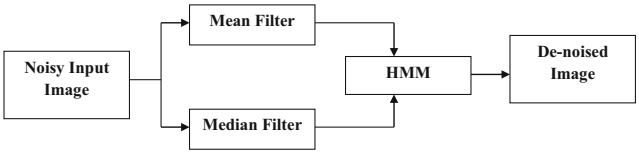

Fig. 4 Illustration of proposed preprocessing using HMM filter

$$s(x,y) = I(x,y) * \delta(x,y) + \partial(x,y) \quad (1)$$

where $s(x, y)$ denotes the speckle noise.

$I(x, y)$ the input image, δ and ∂ are multiplicative and additive components of speckle noise respectively. In the proposed work, the combined effects of mean and median filters are used as a hybrid MM filter to remove the speckle noise as well as to retain the edges.

The 3X3 mask for a sub image, the mean value of 45° neighbours forms an "X" shape and the 90° neighbours forms a "+" shape is shown in Fig. 3. The algorithm is given as follows.

Algorithm:

Step 1: Compute the mean value of the 45° and 90° neighbours and consider as M_{mask}

Step 2: Compute the mean value of the diagonal elements $(i-1, j-1)$, $(i-1, j+1)$, (i, j), $(i+1, j-1)$, $(i+1, j+1)$,and consider as M_{diag}

Step 3: Compute the median value of the diagonal elements $(i-1, j-1)$, $(i-1, j+1)$, (i, j), $(i+1, j-1)$, $(i+1, j+1)$,and consider as Med_{diag}

Step 4: Assume the center pixel (i, j) as C

Step 5: Determine the filtered output $HMM = median(M_{mask}, M_{diag}, Med_{diag}, C)$

The Hybrid MM filtering process is illustrated in a simple diagram and shown Fig. 4. The computation time required for median filter is O (N log N), due to sub mask the computation time is reduced further.

After preprocessing the image is segmented and features extracted which are used to provide the reconstructed image. In case of the proposed fetal kidney segmentation, the position, size, and length of kidneys are taken as the key attributes for abnormality detection.

Segmentation in the proposed work is done by exploiting the clustering features inside a fetal kidney image giving rise to Fuzzy C - means clustering algorithm. Given an image under study, the objective function of Fuzzy C means is defined as

$$I_m(x,y) = \sum_1^m \sum_1^n p_{i,k}{}^l \|x_k - c_i\|^2 \quad (3)$$

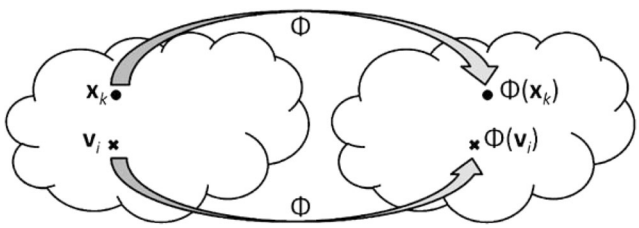

Fig. 5 Feature space and kernel space in kernel based FCM

Where m is the fuzzy weighting index, p denotes the partition matrix and c_i denotes the cluster center, k denotes the iteration steps. The basic principle underlying FCM is that it partitions the input vector set x into fuzzy subsets with p denoting the membership function. However, FCM is very effective provided that the input data set is simple and spherical in nature.

The squared error term in (3) aims to minimize the objective function $I_m(x, y)$. In order to overcome the drawback of FCM, a biased FCM is derived by taking data points close to the centroids of similar patterns while discarding data points far away from the centroid. The far data points are characterized by a low value of membership function. The Eq. (1) can be remodified as

$$I_{mb}(x,y) = \sum_1^m \sum_1^n p_{i,k}{}^l \|x_k - c_i\|^2 + \frac{\delta}{C} \sum_1^n p_{i,k}{}^l \|x_k - c_i\|^2 \quad (4)$$

From the equation (4) δ denotes the controlling parameter of the neighbor window function C and the term $\|x_k - c_i\|$ denote the Euclidean distance. In this proposed work, a Kernel-based FCM (KFCM) is utilized which replaces the Euclidean distance with the Gaussian radial function $1-e^{\frac{\|x_k - c_i\|^2}{\sigma^2}}$. Given a set of feature vector set $S = \{S_1, S_2, S_3, S_4 \ldots S_p\} \in R_n$, the objective function can be arrived as

$$I_{mK}(x,y) = \sum_1^m \sum_1^n p_{i,k}{}^l \|\varnothing(x_k) - \varnothing(c_i)\|^2 \quad (5)$$

The main advantage of Kernel based clustering is implicit mapping between the kernel space and feature space and it is depicted in Fig. 5.

Utilizing the replacement term for Euclidean distance mentioned above, (5) can be rewritten as

$$I_{mK}(x,y) = \sum_1^m \sum_1^n p_{i,k}{}^l (1 - K(x_k, c_i)) \quad (6)$$

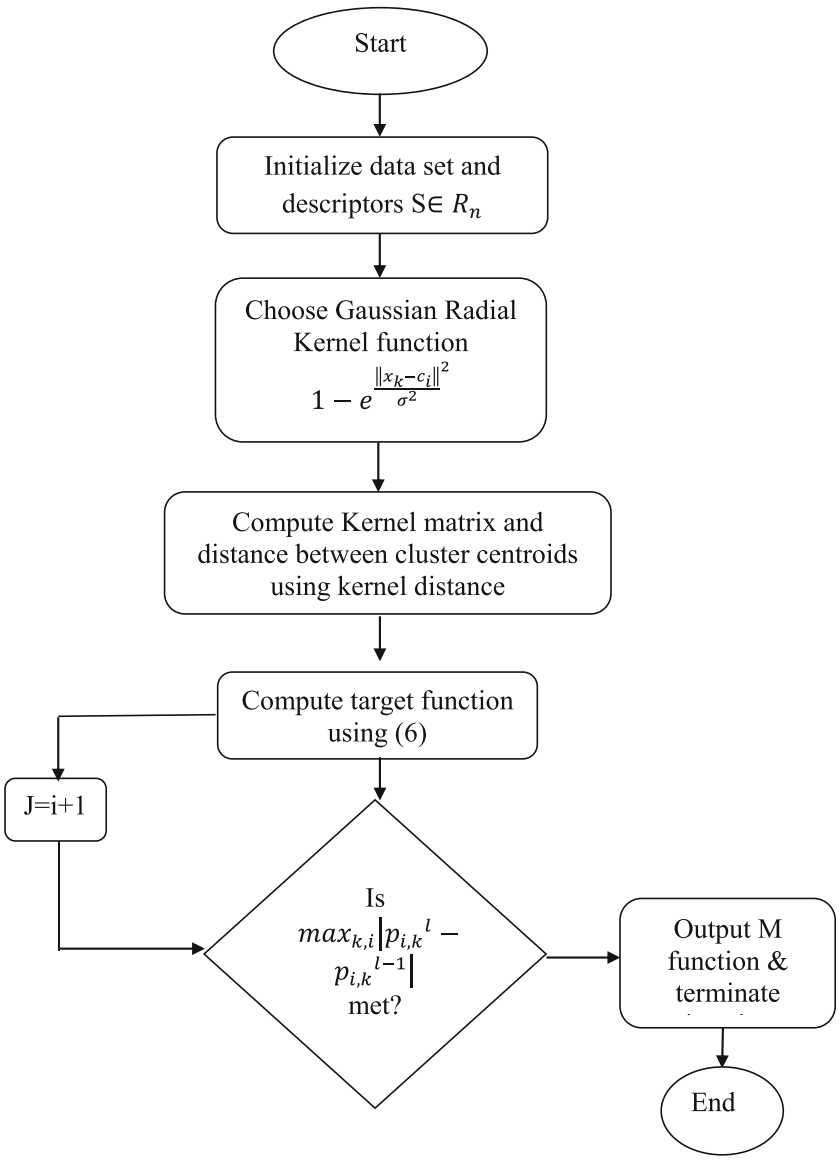

Fig. 6 Flow process of proposed Kernel-based FCM (KFCM) for fetal segmentation

Further the improved equation for the membership term $p_{i,k}$ is derived as

$$p_{i,k} = \frac{\frac{1}{1-K(x_k,c_i)}^{\frac{1}{l-1}}}{\sum \frac{1}{1-K(x_k,c_i)}^{\frac{1}{l-1}}} \quad (7)$$

The update of c_i is given as

$$c_i = \frac{\sum {p_{i,k}}^l K(x_k, c_i) x_k}{\sum {p_{i,k}}^l K(x_k, c_i)} \quad (8)$$

The pseudo code of the KFCM for the proposed implementation is given below along with the flowchart depicted in Fig. 6.

Input: *Input Descriptor set* $S = \{S_1, S_2, S_3, S_4 \ldots S_p\} \in R_n$

Output: *Extracted stream* $C_i = \{C_p, C_{pq}, \ldots \ldots C_{p+q+r\ldots}\} \in P$

Procedure

Generate candidate patterns $P \in P_1 \cap P_2 \cap P_3 \cap \ldots\ldots \cap P_n$

Assign seed = { }

Initialize number of cluster, k.

Apply $Cnd\_Ptrn = P_p \cap P_n$

for t = 1 to r where $P_t \in P(x, y)$

{

for all pixels (i, j) $\in P_p$

for i=0 to $P_t - 1$

do

for j=i+1 to P_t

do

update $p_{i,k}$ *according to (5)*

update c_i *as per (6)*

end if

end for

Return Cnd_Ptrn

Compute $Conf_{measure} = max_{k,i} \left| {p_{i,k}}^l - {p_{i,k}}^{l-1} \right|$

Repeat the update steps until e(t) $\doteqdot 0$.

Group the clusters into $C_i = \{C_p, C_{pq}, \ldots \ldots C_{p+q+r\ldots}\} \in P$

}

end if

end

end procedure

Results and Discussion

The proposed algorithm is tested in MATLAB 17.1 in the operating system of Windows 7 Intel I5 processor with the fetal dataset of 50 images. The Dataset is obtained from Ultrasound Image (US) Database normal features and also the images with abnormalities. The abnormalities are observed by comparing the physical structure, and time duration for the growth. The Bilateral renal agenesis is characterized by absence of kidney, and infantile polycystic kidney disease is viewed as enlarged kidneys are the two factors considered for abnormality detection.

Figure 7a shows the noisy input fetal Ultrasound right side kidney image at third trimester and its de-noised output image using 3 × 3 Hybrid MM filter is shown in Fig. 7b.The performance of the proposed Hybrid MM filter has been quantitatively and qualitatively analyzed using the following measures.

(a) **Mean Square Error (MSE):**

Assume the denoised image is g with respect to the original image f then the MSE.

value is given by

$$MSE = \frac{1}{MN}\sum_{i=0}^{MN-1}(f(i)-g(i))^2 \tag{9}$$

Signal to Noise Ratio (SNR)

The efficiency of denoising method is normally estimated using SNR [24] and described as

$$SNR = 10\log_{10}\frac{\frac{1}{MN}\sum_{i=0}^{MN-1}\left(f(i)^2-g(i)^2\right)^2}{\frac{1}{MN}\sum_{i=0}^{MN-1}(f(i)-g(i))^2} \tag{10}$$

(b) **Structural Similarity Index Measure (SSIM):**

It is a method used to measure the structural similarity between two images [25]. Assume the patches of original and denoised image as x and y.

$$SSIM(x,y) = \frac{\left(2\mu_f\mu_g + C_1\right)\left(2\sigma_{fg} + C_2\right)}{\left(\mu_f{}^2 + \mu_g{}^2 + C_1\right)\left(\sigma_f{}^2 + \sigma_g{}^2 + C_2\right)} \tag{11}$$

μ_f and μ_g are average gray values and σ_f^2 and $\sigma_g{}^2$ are variances. The parameters C_1 and C_2 are constants. The edge-preserving metrics of the proposed HMM filter has been analyzed with the spatial filters such as Mean, Median, Wiener, Lee, Frost and Geometric Filter as listed in Table 1. It is observed that Hybrid MM filter has minimum Mean Square Error (MSE) and low Signal to Noise Ratio (SNR).

Following pre-processing, the KFCM algorithm is applied to the fetal US image to segment the Region of Interest (ROI). Figure 8 depicts the complete segmentation process using the proposed KFCM algorithm.

From the above figure, it is seen that the first image 8(a) depicts the input fetal kidney image at 36th weeks of gestation. The ROI detected results has been depicted in 8(b). The blue curve indicates the ROI extraction using proposed KFCM while the pink region denotes manual ROI descriptor-based extraction.

Figure 8c denotes the rough segmented crude image, the boundary of the method is not well-defined. A texture based boundary detection operator provides the fine-tuned segmented output. Following this segmented output, the features are extracted from the segmented and boundary detected output.

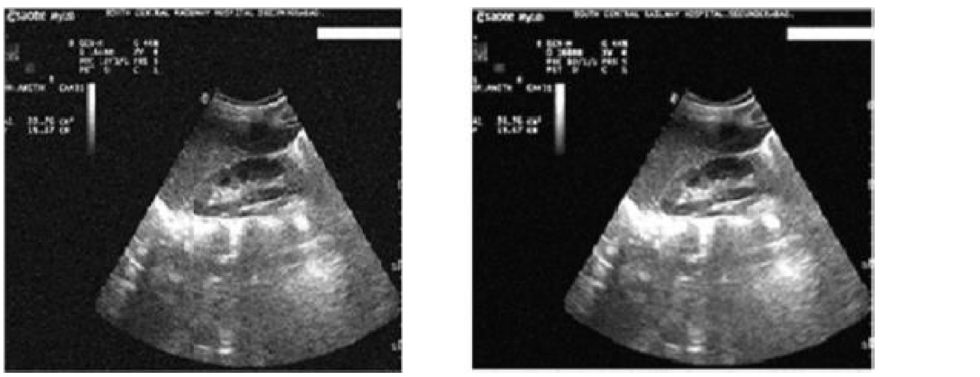

(a) Fetal kidney image **(b) De-noised Fetal Image (3x3 mask)**

Fig. 7 **a** Fetal kidney image, **b** De-noised Fetal Image (3 × 3 mask)

Table 1 Evaluation of edge-preserving parameters

Filter	MSE	SNR (dB)	Structural Similarity Index Measure (SSIM)
Mean	138.44	28.41	0.804
Median	124.22	29.55	0.844
Wiener	108.41	30.14	0.876
Lee	100.78	28.97	0.892
Frost	120.62	27.32	0.886
Geometric	95.55	29.48	0.849
HMM	61.44	34.25	0.921

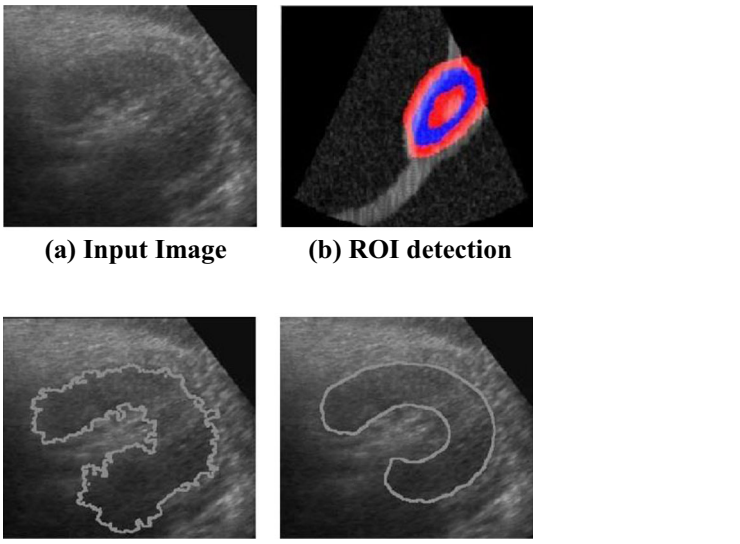

Fig. 8 **a** Input Image **b** ROI detection **c** rough segmented kidney **d** fine tuned segmented kidney output

The common features are listed below.

$$Mean = \frac{1}{MN}\sum X(i,j) \tag{12}$$

$$Skewness = \frac{1}{MN}\sum \frac{\left(X(i,j) - mean\right.}{\delta^3} \tag{13}$$

$$Kurtosis = \frac{1}{MN}\sum \frac{\left(X(i,j) - mean\right.}{\delta^3} \tag{14}$$

$$\text{Correlation} = \sum \frac{(i*j)*P(i,j) - \left(mean_x * mean_y\right)}{\delta_x \delta_y} \tag{15}$$

$$\text{homogenity} = \sum \frac{P(i,j)}{1 + |i-j|}$$

The feature metrics for a healthy fetal kidney condition are specified as mean of 1.08 - 1.336, skewness value of 2.822 - 7.708, Kurtosis of 11.06 - 71.152, homogeneity values ranging from 0.933 to 0.969, a correlation factor of 0.971 - 0.987 placed at Based on the normal feature metrics defined in Table 2, the abnormality is detected.

The comprehensive list of features extracted along with their numerical values is presented in Table 2. These values have been computed and presented for a sample specimen of 10 images. The images have been

Table 2 Extracted feature values from fetal images (Second Trimester)

Image sample/Metric	IMG_001	IMG_075	IMG_084	IMG_094	IMG_102	IMG_143	IMG_168	IMG_179	IMG_188	IMG_200
Mean	1.10	1.14	1.13	1.14	1.06	1.00	1.47	1.28	1.14	1.21
Kurtosis	11.99	14.55	44.01	51.87	10.88	9.98	74.55	64.54	50.87	58.44
Skewness	2.94	3.41	5.66	5.47	1.98	1.64	7.41	4.44	5.14	6.98
Homogeneity	0.94	0.95	0.95	0.94	0.97	0.97	0.92	0.94	0.94	0.94
Correlation	0.97	0.98	0.97	0.98	0.95	0.95	0.99	0.97	0.97	0.97

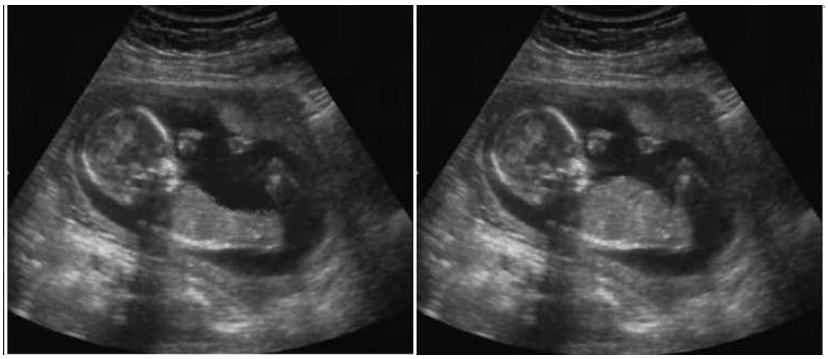

(a) 28th week of gestation (540x480) **(b) 36th week of gestation (540x480)**

Fig. 9 **a** 28th week of gestation (540 × 480), **b** 36th week of gestation (540 × 480)

labeled from 001 to 200 and a set of two images have been depicted in Fig. 9. It is observed that based on the reference measurement values the abnormalities detected in IMG-102, IMG-143 and IMG-168.Further measuring the length and volume of the fetal kidney detects the specific abnormality.

Accuracy assessment is mainly needed to classify the outputs and to compare with different algorithms. The performance is mainly compared with the weight constant 뭔 and the weight assigned to each kernel λ. Entropy is the parameter mainly used to access the quality of based on output and it is less sensitive to parameter variations. The Entropy value can be calculated from the equation [26].

$$Entropy(E) = \sum_{i=1}^{N} \sum_{j=1}^{C} \mu_{ij} \log\left(\mu_{ij}\right) \tag{16}$$

where.

N is the number of pixels in the image
C is the number of classes
μ_{ij} is the membership value

Figure 10a shows the entropy values for different weight constant at 28th week of gestation and Fig. 10b shows the entropy values for different weight constant at 36th week of gestation. It is observed that the weight constant ranging from the value 4 to 8 produces a constant output. Hence it is preferable to choose the weight constant as 4 to 8 for fetal kidney images.

It could be seen from Table 3 that the proposed KFCM is able to compute the maximum number of optimal cluster numbers which accounts for the increased accuracy reported and depicted in Fig. 11. It is observed that the KFCM technique provides a maximum accuracy at third trimesters.

The accuracy comparison with different kernel types kernel in some second and third trimester of gestation has been given in the Table 4. It is observed the compared to other kernel Gaussian Radial Function kernel gives high accuracy at different weeks of gestation.

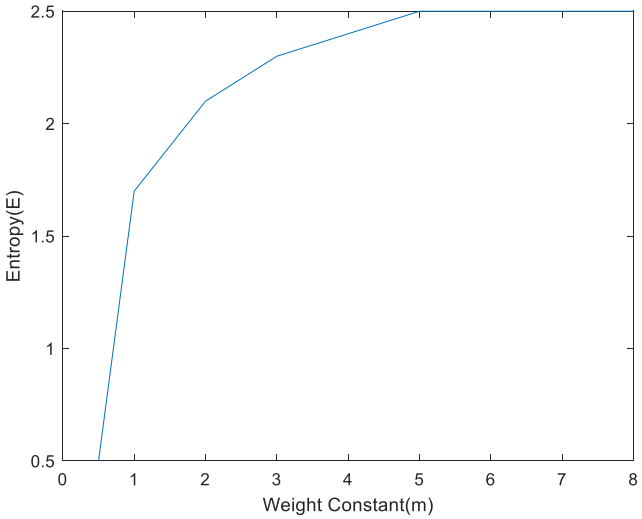

(a) At 28th week of gestation

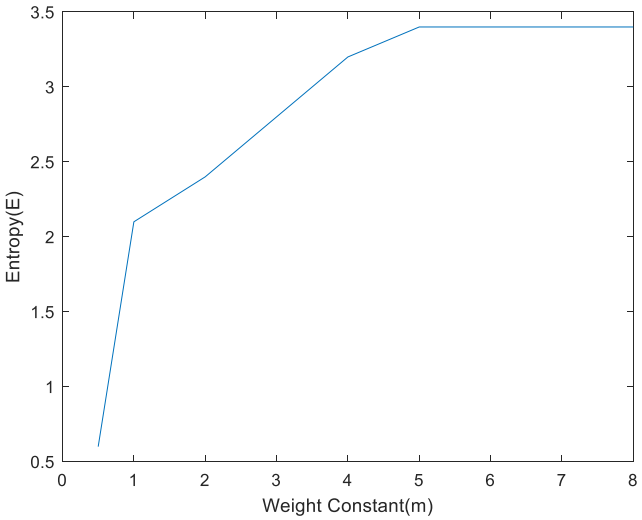

(b) At 36th week of gestation

Fig. 10 Entropy with respect to weight constant at 28th and 36th week of gestation

Table 3 Computation of best cluster–comparative analysis

Sample Image	FCM	PFCM	KFCM	Type-2 Fuzzy C-Means (T2FCM)	Intuitionistic Fuzzy C-Means (IFCM)
20th week of gestation	0.77	0.71	0.76	0.73	0.75
26th week of gestation	0.74	0.80	0.80	0.72	0.78
28th week of gestation	0.74	0.82	0.82	0.81	0.78
32th week of gestation	0.84	0.84	0.81	0.78	0.82
34th week of gestation	0.74	0.86	0.86	0.76	0.80

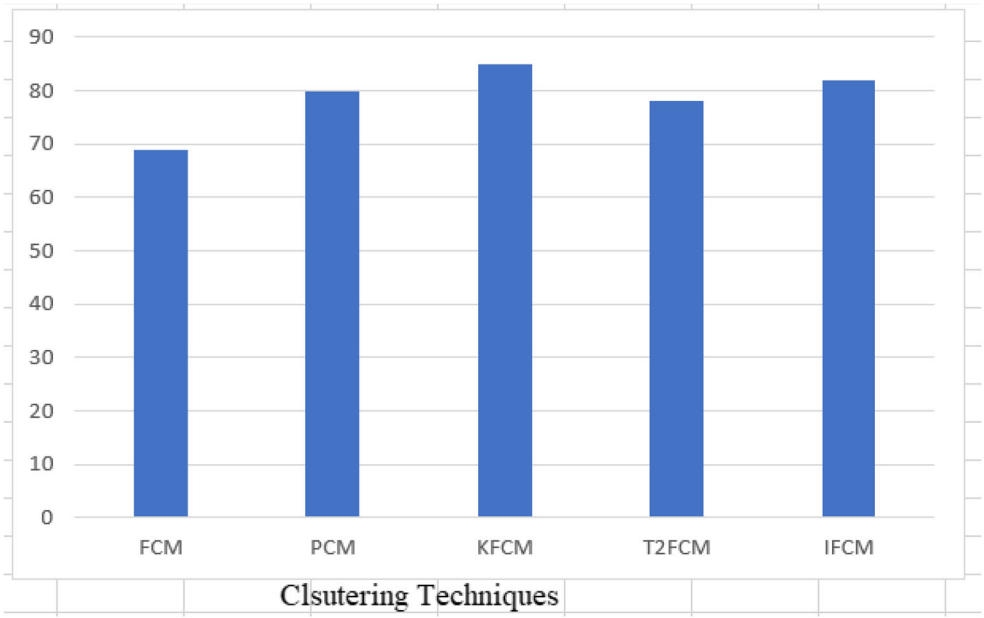

Fig. 11 Performance comparison of segmentation accuracy

The similarity between a threshold binary image (B) and Ground truth image (G) obtained from Jaccard Index and it is given by [27].

$$JaccardIndex = -\frac{|Bi \cap Gi|}{|Bi \cup Gi|} \tag{17}$$

Dice coefficient The Dice coefficient [28] between the threshold binary image (B) and Ground truth image (G) is given as

$$Dicecoefficent = \frac{2|Bi \cup Gi|}{|Bi| + |Gi|} \tag{18}$$

It measures the similarity between two images and gives the overall segmentation quality.

The Dice coefficient and Jaccard Index value at different weeks of gestation has been present in the Table 5.

It is observed that the predicted and truth image has high similarity values at the third trimester compared to the second trimester.

Table 4 Performance comparison of segmentation with different kernels

Kernel used	28th week of gestation	34th week of gestation	36th week gestation
Euclidean Norm	72.3	75.8	78
Polynomial	65.2	69	72.3
Sigmoid	70.5	72.3	78
Gaussian Radial Function (Proposed Method)	80.2	82.9	85.6

Table 5 Similarity Analysis at different weeks of gestation

Gestation in weeks	Dice coefficient	Jaccard Index
20th week	0.49	0.41
26th week	0.49	0.42
28th week	0.50	0.48
32th week	0.53	0.51
34th week	0.53	0.56

Conclusion

The proposed work has been investigated with 50 ultrasound fetal images with the problem formulation to segment and detect congenital disorders by analyzing kidney images as well to predict the gestation period. The Hybrid MM filter have high SNR and low MSE compared with other methods. The segmentation has been done using a derivative of the well known fuzzy C means clustering by replacing the Euclidean distance with a Gaussian Radial kernel function which helps to better approximate complex and non-spherical models. The performance analysis of the proposed method has been compared with different FCM models. It is found to exhibit superior performance over the other two in terms of computation time and precision expressed as accuracy. The experimentation has been done for two cases namely second and third trimesters with the observed values. It is compared against standard coefficient metrics to determine abnormality. The similarity measures also been predicted with Jaccard Coefficient, it shows that a better noise detection technique is needed further improvement in the accuracy of the system.

Compliance with Ethical Standards

Conflict of Interest S.Meenakshi has no conflict of interest with Co-Authors M. Suganthi and P. Suresh Kumar. No conflict of Interest between Three Authors.

Ethical Approval This article does not contain any studies with human participants or animals performed by any of the authors.

Informed Consent As this article does not involve Human participants so, no such informed consent.

References

1. Grandjean, H., Larroque, D., and Levi, S., The performance of routine ultrasonographic screening of pregnancies in the Euro fetus Study. Am. J. Obstet. Gynecol. 181:446–454, 1999.
2. Chen, Y.-N., and Chen, C.-P., Prenatal Ultrasound Evaluation and Outcome of Pregnancy with Fetal Cystic Hygromas and Lymphangiomas. Journal of Medical Ultrasound 25(1), 2017.
3. Reddy, U. M., Filly, R. A., and Copel, J. A., Prenatal Imaging: Ultrasonography and Magnetic Resonance Imaging. Obstet. Gynecol. 112(1):145–157, 2008.
4. Yosypiv, I. V., Congenital anomalies of the kidney and urinary tract: A genetic disorder. International Journal of Nephrology 2012:2020, 2012.
5. Wieczorek, A. P., Wozniak, M. M., and Tyloch, J. F., Errors in the ultrasound diagnosis of the kidneys, ureters and urinary bladder. Journal of Ultrasonography 13:308–318, 2013.
6. Razman, N. R. et al., Filtering Technique in Ultrasound for Kidney, Liver and Pancreas Image using MATLAB. IEEE Student Conference on Research and Development:402–406, 2015.
7. Hafizah, W. M., and Supriyanto, E., Comparative Evaluation of Ultrasound Kidney Image Enhancement Techniques. Journal of Computer Applications 7(21):15–19, 2011.
8. Caliope, P. B., Medeiros, F. N. S., Marques, R. C. P., and Costa, R. C. S., A Comparison of Filters for Ultrasound Images. Telecommunications and Networking 3124:1035–1040, 2004.
9. Jyoti Jaybhay and Rajveer Shastri, "A study of speckle noise reduction filters", Signal & Image Processing: An International Journal (SIPIJ) Vol.6, No.3, June 2015
10. Nobi, M. N., and Yousuf, M. A., A New Method to Remove Noise in Magnetic Resonance and Ultrasound Images. J. Sci. Res. 3(1): 81–89, 2011.
11. Singh, K., and Kaur, S., Ranade, Chandan Singh, "A hybrid algorithm for speckle noise reduction of ultrasound images". Comput. Methods Prog. Biomed. 55-69, 2017.
12. Khare, P., and Mittal, N., Analysis of Medical Image Segmentation Techniques. International Bulletin of Mathematical Research 02(1), 2015.
13. Marsousi, M., Plataniotis, K. N., and Stergiopoulos, S., Shape-Based Kidney Detection and Segmentation in Three-Dimensional Abdominal Ultrasound Images: 36th Annual International Conference of the IEEE Engineering in Medicine and Biology Society, Chicago, 2014.
14. Xie, J., Jiang, Y., and Tsui, H.-T., Segmentation of Kidney from Ultrasound Images Based on Texture and Shape Priors. IEEE Trans. Med. Imaging 24(1), 2005.
15. Song, H., Kang, W., Zhang, Q., and Wang, S., Kidney segmentation in CT sequences using SKFCM and improved Grow Cut algorithm. San Diego: IEEE International Conference on Bioinformatics and Biomedicine, Belfast, 2014.
16. Chen, Y.-T., Medical Image Segmentation Using Independent Component Analysis-Based Kernelized Fuzzy 픰-Means Clustering. Hindawi: Mathematical Problems in Engineering, 2017.
17. Dasa, A., and Sabutb, S. K., Kernelized fuzzy C-means clustering with adaptive thresholding for segmenting liver tumors. Procedia Computer Science, Elsevier 92:389–395, 2016.
18. Bezdek, J. C., Pattern Recognition with Fuzzy Objective Function Algorithm, Plenum, 1981.
19. Kaur, P., Gupta, P., and Sharma, P., Review and Comparison of Kernel Based Fuzzy Image Segmentation Techniques. International Journal of Intelligent Systems and Applications 7: 50–60, 2012.
20. Parasar, D., and Rathod, V. R., Particle swarm optimization K-means clustering segmentation of fetus ultrasound image. International Journal of Signal and Imaging Systems Engineering 10, 2017.
21. Kop, A. M. et al., Kidney Segmentation from Ultrasound Images using Gradient Vector Force. Recent Trends in Image Processing and Pattern Recognition 10(6):1542–1546, 2013.
22. Kaur, P., et al., Kernelized Type-2 Fuzzy C-Means Clustering Algorithm in Segmentation of Noisy Medical Images. IEEE, 2011.
23. Xie, J. et al., Segmentation of Kidney from Ultrasound Images Based on Texture and Shape Priors. IEEE Trans. Med. Imaging 24(1):2202–2210, 2005.
24. Sakrison, D., On the role of the observer and a distortion measure in image transmission. IEEE Transaction on Communication:1251–1267, 1977.

25. Wang, Z., Bovik, A. C., and Sheikh, H. R., Image quality assessment from error visibility to structural similarity. IEEE Transaction on Image Processing:600–612, 2004.
26. Dehghan, H., and Ghassemian, H., Measurement of uncertainty by the entropy : application to the classification of MSS data. Int. J. Remote Sens. 27(18):4005–4014, 2006.
27. Narayana, C., Sreenivasa Reddy, E., and Seetharama Prasad, M., Automatic image segmentation using Ultra fuzziness. Int. J. Comput. Appl. 49(12):6–13, 2012.
28. Dice, L., Measures of the amount of ecologic association between species. Ecology 26:297–302, 1945.